JWKB Method as an Exact Technique

HUJUN SHEN, HARRIS J. SILVERSTONE

Department of Chemistry, The Johns Hopkins University, Baltimore, MD 21218

Received 11 December 2002; accepted 10 October 2003
Published online 25 February 2004 in Wiley InterScience (www.interscience.wiley.com).
DOI 10.1002/qua.20029

ABSTRACT: The JWKB method involves divergent asymptotic expansions in powers of $\hbar$. Borel summability turns divergence into convergence, leading to exact solutions of the Schrödinger equation. The formulas that connect real solutions across linear turning points, where the terms of the expansion are singular, are complex but nonunidirectional. A series of basic problems constructed from linear potentials—for which the JWKB solutions are simple, in which the boundary conditions and physics differ, but for which the turning points are the same—is used to demonstrate the nondirectionality of the turning points and how "Borel sum approximants" lead to exact energy eigenvalues. © 2004 Wiley Periodicals, Inc. Int J Quantum Chem 99: 336–352, 2004

Key words: JWKB; connection formula; Borel sum; asymptotic expansion; semiclassical; double well; tunneling ionization

I. Introduction

It has been known for many years that the JWKB connection formulas at a linear turning point can be completely understood from the Borel summability of the asymptotic expansions of the underlying Airy functions that solve the Schrödinger equation for a linear potential, and that the connection formulas are both complex and nondirectional [1]. Nevertheless, a recent publication [2] by two sensor JWKB specialists erroneously asserts that ". . . when one uses truncated asymptotic series . . . the connection formulas . . . are inherently one-directional" and ". . . Silverstone's Eqs. (24) and (25) [connection formulas] are not correct connection formulas." It would seem that there is a need for simple, clear, concrete examples that demonstrate both the correctness and nondirectionality of the connection formulas [1].

We formulate a set of three problems with two linear turning points, constructed entirely from linear potentials, but that differ in the boundary conditions and physics: scattering, tunneling ionization, and double well, the potentials for which are shown in Figure 1. One can solve the Schrödinger equation for each of these exactly and also by the JWKB method term by term in closed form. For the JWKB method, the different boundary conditions on either side can only both be taken into account if the information flows through the turning points in both directions. Inherent in the demonstration is the implementation of Borel summability for truncated expansions, yielding numerical results that approach the exact.

Correspondence to: H. J. Silverstone; e-mail: hjsilverstone@jhu.edu

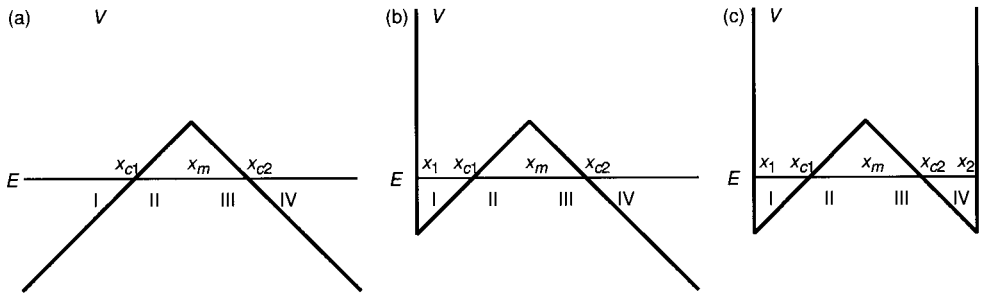

FIGURE 1. Potentials for (a) scattering, (b) tunneling ionization/resonant scattering, and (c) double well.

2. Exact Wave Function

Consider the Schrödinger equation for an "inverted V" potential

$$V(x) = V_0 - k|x - x_m|, \tag{1}$$

with classical turning points (when $E < V_0$),

$$x_{c1} = x_m - (V_0 - E)/k, \tag{2}$$

$$x_{c2} = x_m + (V_0 - E)/k. \tag{3}$$

For $x < x_m$, $V(x)$ is linearly increasing

$$\left(-\frac{\hbar^2}{2m}\frac{d^2}{dx^2} + kx + V_0 - E - kx_m\right)\psi(x) = 0, \tag{4}$$

and the exact wave function is a linear combination of Airy functions:

$$\psi(x) = \psi_1(x) = a_1 \mathrm{Ai}\left[\left(\frac{2mk}{\hbar^2}\right)^{1/3}(x - x_{c1})\right] + b_1 \mathrm{Bi}\left[\left(\frac{2mk}{\hbar^2}\right)^{1/3}(x - x_{c1})\right]. \tag{5}$$

For $x > x_m$, $V(x)$ is linearly decreasing

$$\left(-\frac{\hbar^2}{2m}\frac{d^2}{dx^2} - kx + V_0 - E + kx_m\right)\psi(x) = 0. \tag{6}$$

The exact wave function is again a linear combination of Airy functions:

$$\psi(x) = \psi_2(x) = a_2 \mathrm{Ai}\left[\left(\frac{2mk}{\hbar^2}\right)^{1/3}(x_{c2} - x)\right] + b_2 \mathrm{Bi}\left[\left(\frac{2mk}{\hbar^2}\right)^{1/3}(x_{c2} - x)\right]. \tag{7}$$

2.1. MATCHING AT $x = x_m$

At $x = x_m$, both $\psi_1(x_m) = \psi_2(x_m)$ and $\psi_1'(x_m) = \psi_2'(x_m)$, which implies a linear relationship between the coefficients $\{a_1, b_1\}$ and $\{a_2, b_2\}$. We introduce a parameter κ, which when $\hbar = 2m = 1$ will be the same as k but otherwise permits us to keep track of powers of $\hbar$:

$$\kappa = \hbar k/\sqrt{2m}. \tag{8}$$

Then, the following matching conditions are common to all the examples treated below—distinguished from each other by different boundary conditions:

$$a_1 = -a_2\pi\kappa^{2/3}\frac{d}{dE}(\mathrm{Bi}[\kappa^{-2/3}(V_0 - E)]\mathrm{Ai}[\kappa^{-2/3}(V_0 - E)]) - b_2\pi\kappa^{2/3}\frac{d}{dE}\mathrm{Bi}[\kappa^{-2/3}(V_0 - E)]^2, \tag{9}$$

$$b_1 = +a_2\pi\kappa^{2/3}\frac{d}{dE}\mathrm{Ai}[\kappa^{-2/3}(V_0 - E)]^2 + b_2\pi\kappa^{2/3}\frac{d}{dE}(\mathrm{Bi}[\kappa^{-2/3}(V_0 - E)]\mathrm{Ai}[\kappa^{-2/3}(V_0 - E)]), \tag{10}$$

and, symmetrically,

$$a_2 = -a_1\pi\kappa^{2/3}\frac{d}{dE}\,(\mathrm{Bi}[\kappa^{-2/3}(V_0 - E)]\mathrm{Ai}[\kappa^{-2/3}(V_0 - E)]) - b_1\pi\kappa^{2/3}\frac{d}{dE}\,\mathrm{Bi}[\kappa^{-2/3}(V_0 - E)]^2, \quad (11)$$

$$b_2 = +a_1\pi\kappa^{2/3}\frac{d}{dE}\,\mathrm{Ai}[\kappa^{-2/3}(V_0 - E)]^2 + b_1\pi\kappa^{2/3}\frac{d}{dE}\,(\mathrm{Bi}[\kappa^{-2/3}(V_0 - E)]\mathrm{Ai}[\kappa^{-2/3}(V_0 - E)]). \quad (12)$$

3. JWKB Wave Functions

The exact wave function has two parts, $\psi_1(x)$ for $x < x_m$ and $\psi_2(x)$ for $x > x_m$. The JWKB wave function has four parts. There are two classically allowed regions (I and IV: $x < x_{c1}$ and $x_{c2} < x$) and two classically forbidden regions (II and III; $x_{c1} < x \le x_m$ and $x_m \le x < x_{c2}$), as labeled in Figure 1. The JWKB wave function in each of these four regions is given by

$$\psi_{\mathrm{I}}(x) = c_{\mathrm{I}}(-dS_{\mathrm{I}}/dx)^{-1/2}e^{i(S_{\mathrm{I}}/\hbar+\pi/4)} + d_{\mathrm{I}}(-dS_{\mathrm{I}}/dx)^{-1/2}e^{-i(S_{\mathrm{I}}/\hbar+\pi/4)} \quad (13)$$

$$\psi_{\mathrm{II}}(x) = c_{\mathrm{II}}(dQ_{\mathrm{II}}/dx)^{-1/2}e^{Q_{\mathrm{II}}/\hbar} + d_{\mathrm{II}}(dQ_{\mathrm{II}}/dx)^{-1/2}e^{-Q_{\mathrm{II}}/\hbar}. \quad (14)$$

$$\psi_{\mathrm{III}}(x) = c_{\mathrm{III}}(-dQ_{\mathrm{III}}/dx)^{-1/2}e^{Q_{\mathrm{III}}/\hbar} + d_{\mathrm{III}}(-dQ_{\mathrm{III}}/dx)^{-1/2}e^{-Q_{\mathrm{III}}/\hbar} \quad (15)$$

$$\psi_{\mathrm{IV}}(x) = c_{\mathrm{IV}}(dS_{\mathrm{IV}}/dx)^{-1/2}e^{i(S_{\mathrm{IV}}/\hbar+\pi/4)} + d_{\mathrm{IV}}(dS_{\mathrm{IV}}/dx)^{-1/2}e^{-i(S_{\mathrm{IV}}/\hbar+\pi/4)}. \quad (16)$$

As is characteristic of the JWKB method [3, 4], the "action functions" S_{I}, Q_{II}, Q_{III}, and S_{IV} are expanded in powers of $\hbar^2$:

$$S_{\mathrm{I}} = S_{\mathrm{I}}^{(0)} + \hbar^2 S_{\mathrm{I}}^{(1)} + \hbar^4 S_{\mathrm{I}}^{(2)} + \cdots \quad (17)$$

$$Q_{\mathrm{II}} = Q_{\mathrm{II}}^{(0)} + \hbar^2 Q_{\mathrm{II}}^{(1)} + \hbar^4 Q_{\mathrm{II}}^{(2)} + \cdots \quad (18)$$

$$Q_{\mathrm{III}} = Q_{\mathrm{III}}^{(0)} + \hbar^2 Q_{\mathrm{III}}^{(1)} + \hbar^4 Q_{\mathrm{III}}^{(2)} + \cdots \quad (19)$$

$$S_{\mathrm{IV}} = S_{\mathrm{IV}}^{(0)} + \hbar^2 S_{\mathrm{IV}}^{(1)} + \hbar^4 S_{\mathrm{IV}}^{(2)} + \cdots. \quad (20)$$

For simplicity, we henceforth use units in which $\hbar = 2m = 1$; however, k is to remain explicit and later will be given numerical values and $\hbar$ will on occasion be included in the formulas when helpful to keep track of order.

3.1. EXACT TERM-BY-TERM SOLUTION

We remark that the JWKB $S_{\mathrm{I}}^{(N)}$, $Q_{\mathrm{II}}^{(N)}$, $Q_{\mathrm{III}}^{(N)}$, and $S_{\mathrm{IV}}^{(N)}$ for a linear potential are simple [5]:

$$Q_j^{(0)} = \zeta_j \quad (21)$$

$$Q_j^{(1)} = \frac{5}{72}\,\zeta_j^{-1} \quad (22)$$

$$Q_j^{(N)} = c^{(N)}\zeta_j^{1-2N} \quad (23)$$

$$S_j^{(0)} = \zeta_j \quad (24)$$

$$S_j^{(1)} = -\frac{5}{72}\,\zeta_j^{-1} \quad (25)$$

$$S_j^{(N)} = (-1)^N c^{(N)}\zeta_j^{1-2N}, \quad (26)$$

where $c^{(N)}$ is a rational constant, and

$$\zeta_{\mathrm{I}} = \zeta_{\mathrm{I}}(x, k, x_{c1}) = \frac{2}{3}k^{1/2}(x_{c1} - x)^{3/2} \quad (27)$$

$$\zeta_{\mathrm{II}} = \zeta_{\mathrm{II}}(x, k, x_{c1}) = \frac{2}{3}k^{1/2}(x - x_{c1})^{3/2} \quad (28)$$

$$\zeta_{\mathrm{III}} = \zeta_{\mathrm{III}}(x, k, x_{c2}) = \frac{2}{3}k^{1/2}(x_{c2} - x)^{3/2} \quad (29)$$

$$\zeta_{\mathrm{IV}} = \zeta_{\mathrm{IV}}(x, k, x_{c2}) = \frac{2}{3}k^{1/2}(x - x_{c2})^{3/2}. \quad (30)$$

The perceptive reader might question the choice of integration constants in Eqs. (21)–(26): The JWKB equations determine directly only the derivatives $dS_j^{(N)}/dx$ and $dQ_j^{(N)}/dx$, and the integration constants are (logarithmically speaking) normalization. The motivation, however, is obvious: Preserve the square-root branch point at the turning point. This choice is consistent with the standard way to avoid integrating through the turning point when the integrand is singular,

$$S_j^{(N)}(x) = \frac{1}{2}\int^{(x,x_c^{(\pm)},x)} \frac{dS_j^{(N)}}{dx}\,dx \tag{31}$$

$$Q_j^{(N)}(x) = \frac{1}{2}\int^{(x,x_c^{(\pm)},x)} \frac{dQ_j^{(N)}}{dx}\,dx, \tag{32}$$

where in each case the integration path starts at x, loops around the classical turning point x_c in the sense $(\pm)$ that makes $S_j^{(0)}$ and $Q_j^{(0)}$ respectively positive, and then returns to x. This choice also makes $S_j^{(N)}(x)$ equal $\pm i$ times the analytic continuation of $Q_j^{(N)}(x)$ around the turning point, the sign depending on the sense. Finally, any other choice would have to be undone in, and therefore complicate, the connection formulas (33)–(36).

The simplicity of $S_j^{(N)}$ and $Q_j^{(N)}$ allows us to take expansions to high truncation order $N = N_T$ and permits all attention to be focused on the connection formulas and the Borel summation method.

3.2. CONNECTION FORMULAS

For completeness, we repeat here the connection formulas given previously [1].* When the classically allowed region lies to the left of the turning point, the connection formulas are

$$\begin{aligned}
&(b - ia)(-dS_{\rm I}/dx)^{-1/2}e^{i(S_{\rm I}/\hbar+\pi/4)} \\
&\qquad + (b + ia)(-dS_{\rm I}/dx)^{-1/2}e^{-i(S_{\rm I}/\hbar+\pi/4)}, \\
&\qquad\qquad (-\pi/3 < \arg(x_{c1} - x) < \pi/3), \\
&\leftrightarrow 2b(dQ_{\rm II}/dx)^{-1/2}e^{Q_{\rm II}/\hbar} \\
&\qquad + (a + ib)(dQ_{\rm II}/dx)^{-1/2}e^{-Q_{\rm II}/\hbar}, \\
&\qquad (0 < \arg(x - x_{c1}) < 2\pi/3)[\mathrm{Im}\, x > 0], \quad (33) \\
&\leftrightarrow 2b(dQ_{\rm II}/dx)^{-1/2}e^{Q_{\rm II}/\hbar} \\
&\qquad + (a - ib)(dQ_{\rm II}/dx)^{-1/2}e^{-Q_{\rm II}/\hbar}, \\
&\qquad (-2\pi/3 < \arg(x - x_{c1}) < 0)[\mathrm{Im}\, x < 0]. \quad (34)
\end{aligned}$$

When the classically allowed region lies to the right of the turning point, the connection formulas are

$$\begin{aligned}
&(b - ia)(dS_{\rm IV}/dx)^{-1/2}e^{i(S_{\rm IV}/\hbar+\pi/4)} \\
&\qquad + (b + ia)(dS_{\rm IV}/dx)^{-1/2}e^{-i(S_{\rm IV}/\hbar+\pi/4)}, \\
&\qquad\qquad (-\pi/3 < \arg(x - x_{c2}) < \pi/3), \\
&\leftrightarrow 2b(-dQ_{\rm III}/dx)^{-1/2}e^{Q_{\rm III}/\hbar} \\
&\qquad + (a + ib)(-dQ_{\rm III}/dx)^{-1/2}e^{-Q_{\rm III}/\hbar}, \\
&\qquad (0 < \arg(x_{c2} - x) < 2\pi/3)[\mathrm{Im}\, x < 0], \quad (35) \\
&\leftrightarrow 2b(-dQ_{\rm III}/dx)^{-1/2}e^{Q_{\rm III}/\hbar} \\
&\qquad + (a - ib)(-dQ_{\rm III}/dx)^{-1/2}e^{-Q_{\rm III}/\hbar}, \\
&\qquad (-2\pi/3 < \arg(x_{c2} - x) < 0)[\mathrm{Im}\, x > 0]. \quad (36)
\end{aligned}$$

In Eqs. (33)–(36), a and b can be any complex numbers and the results are for any smooth potential $V(x)$, so long as the turning points are linear.

The proper connection formula here depends on how x is treated in regions II and III, where x lies on Stokes lines [1]. It is necessary to "pick sides." We choose Im $x = +0$, that is, we consider x to belong to the upper half-plane. Then, the connection between regions I and II is given by [Eq. (33)]

$$c_{\rm I} = -id_{\rm II} \tag{37}$$

$$d_{\rm I} = c_{\rm II} + id_{\rm II} \tag{38}$$

and between regions III and IV by [Eq. (36)]

$$d_{\rm IV} = id_{\rm III} \tag{39}$$

$$c_{\rm IV} = c_{\rm III} - id_{\rm III}. \tag{40}$$

3.3. MATCHING CONDITIONS

In each example, the wave functions have to be matched at the point x_m where the increasing potential switches to decreasing,

$$\psi_{\rm II}(x_m + i0) = \psi_{\rm III}(x_m + i0) \tag{41}$$

$$\psi'_{\rm II}(x_m + i0) = \psi'_{\rm III}(x_m + i0), \tag{42}$$

which lead to a linear relation between the coefficients $\{c_{\rm II}, d_{\rm II}\}$ and $\{c_{\rm III}, d_{\rm III}\}$. For clarity, differentiation by x is denoted by an over-dot:

$$\begin{aligned}
c_{\rm II} = &-\frac{1}{2}c_{\rm III}(\dot{Q}_{\rm II})^{-1/2}e^{-Q_{\rm II}/\hbar}(-\dot{Q}_{\rm III})^{-1/2}e^{Q_{\rm III}/\hbar} \\
&\times\left(-\dot{Q}_{\rm II} - \frac{\hbar}{2}\frac{\ddot{Q}_{\rm II}}{\dot{Q}_{\rm II}} - \dot{Q}_{\rm III} + \frac{\hbar}{2}\frac{\ddot{Q}_{\rm III}}{\dot{Q}_{\rm III}}\right)_{x=x_m+i0}
\end{aligned}$$

*From Ref. [5], Eqs. (209) and (211), which pertain explicitly to the case that the classically forbidden region is to the right.

$$-\frac{1}{2}d_{\rm III}(\dot{Q}_{\rm II})^{-1/2}e^{-Q_{\rm II}/\hbar}(-\dot{Q}_{\rm III})^{-1/2}e^{-Q_{\rm III}/\hbar}$$
$$\times\left(-\dot{Q}_{\rm II}-\frac{\hbar}{2}\frac{\ddot{Q}_{\rm II}}{\dot{Q}_{\rm II}}+\dot{Q}_{\rm III}+\frac{\hbar}{2}\frac{\ddot{Q}_{\rm III}}{\dot{Q}_{\rm III}}\right)_{x=x_m+i0}, \quad (43)$$

$$d_{\rm II}=+\frac{1}{2}c_{\rm III}(\dot{Q}_{\rm II})^{-1/2}e^{Q_{\rm II}/\hbar}(-\dot{Q}_{\rm III})^{-1/2}e^{Q_{\rm III}/\hbar}$$
$$\times\left(+\dot{Q}_{\rm II}-\frac{\hbar}{2}\frac{\ddot{Q}_{\rm II}}{\dot{Q}_{\rm II}}-\dot{Q}_{\rm III}+\frac{\hbar}{2}\frac{\ddot{Q}_{\rm III}}{\dot{Q}_{\rm III}}\right)_{x=x_m+i0}$$
$$+\frac{1}{2}d_{\rm III}(\dot{Q}_{\rm II})^{-1/2}e^{Q_{\rm II}/\hbar}(-\dot{Q}_{\rm III})^{-1/2}e^{-Q_{\rm III}/\hbar}$$
$$\times\left(+\dot{Q}_{\rm II}-\frac{\hbar}{2}\frac{\ddot{Q}_{\rm II}}{\dot{Q}_{\rm II}}+\dot{Q}_{\rm III}+\frac{\hbar}{2}\frac{\ddot{Q}_{\rm III}}{\dot{Q}_{\rm III}}\right)_{x=x_m+i0}. \quad (44)$$

If the energy is over the top of the potential, i.e., $E > V_0$, then there are no longer classical turning points. Nevertheless, one can still use the JWKB formalism, as we shall do for the scattering problem, and in this case ψ_1 is directly matched to $\psi_{\rm IV}$ by a direct linear relation between $\{c_{\rm I}, d_{\rm I}\}$ and $\{c_{\rm IV}, d_{\rm IV}\}$,

$$c_{\rm I}=\frac{1}{2}c_{\rm IV}(-\dot{S}_{\rm I})^{-1/2}e^{-iS_{\rm I}/\hbar}(\dot{S}_{\rm IV})^{-1/2}e^{iS_{\rm IV}/\hbar}$$
$$\times\left(+\dot{S}_{\rm I}-\frac{i\hbar}{2}\frac{\ddot{S}_{\rm I}}{\dot{S}_{\rm I}}+\dot{S}_{\rm IV}+\frac{i\hbar}{2}\frac{\ddot{S}_{\rm IV}}{\dot{S}_{\rm IV}}\right)_{x=x_m+i0}$$
$$+\frac{1}{2}d_{\rm IV}(-\dot{S}_{\rm I})^{-1/2}e^{-iS_{\rm I}/\hbar}(\dot{S}_{\rm IV})^{-1/2}e^{-iS_{\rm IV}/\hbar-i\pi/2}$$
$$\times\left(+\dot{S}_{\rm I}-\frac{i\hbar}{2}\frac{\ddot{S}_{\rm I}}{\dot{S}_{\rm I}}-\dot{S}_{\rm IV}+\frac{i\hbar}{2}\frac{\ddot{S}_{\rm IV}}{\dot{S}_{\rm IV}}\right)_{x=x_m+i0}, \quad (E>V_0), \quad (45)$$

$$d_{\rm I}=+\frac{1}{2}c_{\rm IV}(-\dot{S}_{\rm I})^{-1/2}e^{iS_{\rm I}/\hbar}(\dot{S}_{\rm IV})^{-1/2}e^{iS_{\rm IV}/\hbar+i\pi/2}$$
$$\times\left(+\dot{S}_{\rm I}+\frac{i\hbar}{2}\frac{\ddot{S}_{\rm I}}{\dot{S}_{\rm I}}-\dot{S}_{\rm IV}-\frac{i\hbar}{2}\frac{\ddot{S}_{\rm IV}}{\dot{S}_{\rm IV}}\right)_{x=x_m+i0}$$
$$+\frac{1}{2}d_{\rm IV}(-\dot{S}_{\rm I})^{-1/2}e^{iS_{\rm I}/\hbar}(\dot{S}_{\rm IV})^{-1/2}e^{-iS_{\rm IV}/\hbar}$$
$$\times\left(+\dot{S}_{\rm I}+\frac{i\hbar}{2}\frac{\ddot{S}_{\rm I}}{\dot{S}_{\rm I}}+\dot{S}_{\rm IV}-\frac{i\hbar}{2}\frac{\ddot{S}_{\rm IV}}{\dot{S}_{\rm IV}}\right)_{x=x_m+i0}, \quad (E>V_0). \quad (46)$$

4. Formal Solutions

Given the common inverted-V potential [Eq. (1)], the boundary conditions define the problem.

1. Outgoing wave only on the right corresponds to scattering, with incoming and reflected waves on the left. The physical quantity to calculate is the transmission coefficient.
2. A hard wall on the left at $x = x_1$ corresponds to resonant scattering from the right or, equivalently, tunneling ionization from within the "well." The physical quantities to calculate are the resonance positions and widths or the quasistationary energies and tunneling ionization rates.
3. Symmetrically placed hard walls on the left and right at $x = x_1$ and $x = x_2$ corresponds to a double-well potential. The physical quantities of interest are the paired double-well states with their exponentially small energy splittings.

In this section we discuss the analytic aspects of the exact and JWKB solutions. In the following two sections we discuss numerical calculations.

4.1. SCATTERING: TRANSMISSION COEFFICIENT

4.1.1. Exact Solution

The scattering boundary condition, purely outgoing wave on the right, is characterized by

$$\psi_2(x)=\mathrm{Bi}[\kappa^{-2/3}k(x_{c2}-x)]+i\mathrm{Ai}[\kappa^{-2/3}k(x_{c2}-x)] \quad (47)$$

$$b_2=1 \quad (48)$$

$$a_2=i. \quad (49)$$

The *incoming* wave on the left,

$$\psi_{1,\rm incoming}(x)=\mathrm{Bi}[\kappa^{-2/3}k(x-x_{c1})]$$
$$-i\mathrm{Ai}[\kappa^{-2/3}k(x-x_{c1})], \quad (50)$$

then has the coefficient

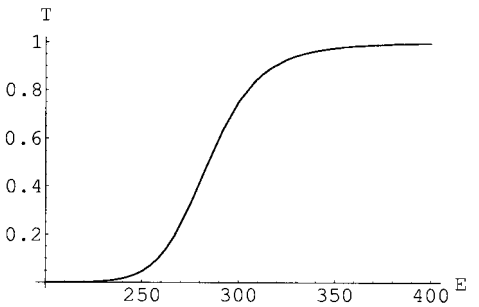

FIGURE 2. Transmission coefficient T when $k = V_0 = 300$.

$$\frac{b_1 + ia_1}{2} = i\pi(\mathrm{Bi}[\kappa^{-2/3}(V_0 - E)] + i\mathrm{Ai}[\kappa^{-2/3}(V_0 - E)])$$

$$\times (\mathrm{Bi}'[\kappa^{-2/3}(V_0 - E)] + i\mathrm{Ai}'[\kappa^{-2/3}(V_0 - E)]). \quad (51)$$

Consequently, the exact transmission coefficient $T_{\mathrm{exact}}(E)$, the squared magnitude of the ratio of the transmitted wave to incoming wave coefficients, is given by

$$1/T_{\mathrm{exact}}(E) = |(b_1 + ia_1)/2|^2 \quad (52)$$

$$= \pi^2(\mathrm{Bi}[\kappa^{-2/3}(V_0 - E)]^2 + \mathrm{Ai}[\kappa^{-2/3}(V_0 - E)]^2)$$

$$(\mathrm{Bi}'[\kappa^{-2/3}(V_0 - E)]^2 + \mathrm{Ai}'[\kappa^{-2/3}(V_0 - E)]^2) \quad (53)$$

$$= 1 + \pi^2(\mathrm{Bi}[\kappa^{-2/3}(V_0 - E)]\mathrm{Bi}'[\kappa^{-2/3}(V_0 - E)]$$

$$+ \mathrm{Ai}[\kappa^{-2/3}(V_0 - E)]\mathrm{Ai}'[\kappa^{-2/3}(V_0 - E)])^2. \quad (54)$$

Formulas (53) and (54) are valid for all values of E. The transmission coefficient is plotted in Figure 2, with $\hbar = 2m = 1$ and $V_0 = k = \kappa = 300$.

4.1.2. JWKB Solution

The purely outgoing wave JWKB solution is characterized by

$$\psi_{\mathrm{IV}}(x) = \dot{S}_{\mathrm{IV}}^{-1/2} e^{i(S_{\mathrm{IV}}/\hbar + \pi/4)} \quad (55)$$

$$c_{\mathrm{IV}} = 1 \quad (56)$$

$$d_{\mathrm{IV}} = 0, \quad (57)$$

and the quantity to calculate is

$$1/T_{\mathrm{JWKB}} = |d_{\mathrm{I}}|^2. \quad (58)$$

[It is of no consequence that the normalization of $\psi_{\mathrm{IV}}(x)$ and $\psi_2(x)$ differ by a factor $\sqrt{\pi}$.]

When the energy is above the top of the barrier, the formula for T_{JWKB} is concise. From Eqs. (58), (56), (57), and (46) we obtain

$$1/T_{\mathrm{JWKB}} = \frac{1}{4}(-\dot{S}_{\mathrm{I}})^{-1}(\dot{S}_{\mathrm{IV}})^{-1}$$

$$\times \left[(\dot{S}_{\mathrm{I}} - \dot{S}_{\mathrm{IV}})^2 + \frac{\hbar^2}{4}\left(\frac{\ddot{S}_{\mathrm{I}}}{\dot{S}_{\mathrm{I}}} - \frac{\ddot{S}_{\mathrm{IV}}}{\dot{S}_{\mathrm{IV}}}\right)^2\right]_{x=x_m}. \quad (59)$$

This last result can be simplified via Eqs. (24)–(27) and (30), the equality *here*

$$x_{c1} - x_m = x_m - x_{c2} \quad (60)$$

$$= (E - V_0)/k, \quad (61)$$

the Borel summability of S_{I} and S_{IV}, and

$$(-\dot{S}_{\mathrm{I}})^n|_{x=x_m} = (\dot{S}_{\mathrm{IV}})^n|_{x=x_m}. \quad (62)$$

Thus, for transmission over the barrier ($E > V_0$),

$$1/T_{\mathrm{JWKB}} = 1 + (\hbar^2/4)\ddot{S}_{\mathrm{I}}^2(-\dot{S}_{\mathrm{I}})^{-4}|_{x=x_m}. \quad (63)$$

When the energy is less than the top, so that the particle tunnels through the barrier, it is necessary to follow the connection $(c_{\mathrm{IV}}, d_{\mathrm{IV}}) = (1, 0)$ [Eqs. (56) and (57)] $\rightarrow (c_{\mathrm{III}}, d_{\mathrm{III}}) = (1, 0)$ [Eqs. (39) and (40)] $\rightarrow$ c_{II} and d_{II} [Eqs. (43) and (44)] $\rightarrow d_{\mathrm{I}} = c_{\mathrm{II}} + id_{\mathrm{II}}$ [Eq. (38)]. Accordingly, one obtains for d_{I}

$$d_{\mathrm{I}} = \frac{i}{2}\dot{Q}_{\mathrm{II}}^{-1/2}(e^{Q_{\mathrm{II}}/\hbar} + ie^{-Q_{\mathrm{II}}/\hbar})(-\dot{Q}_{\mathrm{III}})^{-1/2}e^{Q_{\mathrm{III}}/\hbar}$$

$$\times \left(-\dot{Q}_{\mathrm{III}} + \frac{\hbar}{2}\frac{\ddot{Q}_{\mathrm{III}}}{\dot{Q}_{\mathrm{III}}}\right)\Bigg|_{x=x_m+i0} + \frac{i}{2}\dot{Q}_{\mathrm{II}}^{-1/2}$$

$$\times \left[e^{Q_{\mathrm{II}}/\hbar}\left(+\dot{Q}_{\mathrm{II}} - \frac{\hbar}{2}\frac{\ddot{Q}_{\mathrm{II}}}{\dot{Q}_{\mathrm{II}}}\right) + ie^{-Q_{\mathrm{II}}/\hbar}\left(-\dot{Q}_{\mathrm{II}} - \frac{\hbar}{2}\frac{\ddot{Q}_{\mathrm{II}}}{\dot{Q}_{\mathrm{II}}}\right)\right]$$

$$\times (-\dot{Q}_{\mathrm{III}})^{-1/2}e^{Q_{\mathrm{III}}/\hbar}\Bigg|_{x=x_m+i0}. \quad (64)$$

Just as Eq. (59) could be simplified into Eq. (63), so too can Eq. (64) be simplified. But, the analog of Eq. (62) has a major difference because the Q_j are used on the Stokes line of the asymptotic series. Thus, $\zeta_{\mathrm{III}}(x_m + i0, k, x_{c2})$ and $\zeta_{\mathrm{II}}(x_m + i0, k, x_{c1})$,

while otherwise equal, fall on opposite sides of the Stokes line.

$$\zeta_{\rm II}(x_m + i0, k, x_{c1}) = \frac{2}{3} k^{1/2}(x_m + i0 - x_{c1})^{3/2} \quad (65)$$

$$= \frac{2}{3k} (V_0 - E + i0)^{3/2}, \quad (66)$$

$$\zeta_{\rm III}(x_m + i0, k, x_{c2}) = \frac{2}{3} k^{1/2}(x_{c2} - x_m - i0)^{3/2} \quad (67)$$

$$= \frac{2}{3k} (V_0 - E - i0)^{3/2} \quad (68)$$

$$= \zeta_{\rm II}(x_m - i0, k, x_{c1}), \quad (69)$$

$$\left(- \frac{dQ_{\rm III}}{dx} \right)^n_{x=x_m+i0} = \left(\frac{dQ_{\rm II}}{dx} \right)^n_{x=x_m-i0}. \quad (70)$$

To cross the Stokes line is yet another application of the connection formulas (33)–(36):

$$\dot{Q}_{\rm II}^{-1/2}(e^{Q_{\rm II}/\hbar} + ie^{-Q_{\rm II}/\hbar})_{x=x_m+i0} = \dot{Q}_{\rm II}^{-1/2} e^{Q_{\rm II}/\hbar}\big|_{x=x_m-i0} \quad (71)$$

$$= (-\dot{Q}_{\rm III})^{-1/2} e^{Q_{\rm III}/\hbar}\big|_{x=x_m+i0} \quad (72)$$

$$\dot{Q}_{\rm II}^{-1/2}\left[e^{Q_{\rm II}/\hbar}\left(+\dot{Q}_{\rm II} - \frac{\hbar}{2}\frac{\ddot{Q}_{\rm II}}{\dot{Q}_{\rm II}} \right) + ie^{-Q_{\rm II}/\hbar}\left(-\dot{Q}_{\rm II} - \frac{\hbar}{2}\frac{\ddot{Q}_{\rm II}}{\dot{Q}_{\rm II}} \right) \right]_{x_m+i0} = \dot{Q}_{\rm II}^{-1/2} e^{Q_{\rm II}/\hbar}\left(\dot{Q}_{\rm II} - \frac{\hbar}{2}\frac{\ddot{Q}_{\rm II}}{\dot{Q}_{\rm II}} \right)_{x_m-i0} \quad (73)$$

$$= (-\dot{Q}_{\rm III})^{-1/2} e^{Q_{\rm III}/\hbar}\left(-\dot{Q}_{\rm III} + \frac{\hbar}{2}\frac{\ddot{Q}_{\rm III}}{\dot{Q}_{\rm III}} \right)_{x_m+i0}. \quad (74)$$

Thus, Eq. (64) for $d_{\rm I}$ can be put in the simpler form,

$$d_{\rm I} = ie^{2Q_{\rm III}/\hbar}\left(1 - \frac{\hbar}{2}\ddot{Q}_{\rm III}\dot{Q}_{\rm III}^{-2} \right)_{x=x_m+i0}, \quad (75)$$

which leads directly to the JWKB transmission coefficient [vs. the exact result in Eq. (53)]

$$1/T_{\rm JWKB} = \left| e^{2Q_{\rm III}/\hbar}\left(1 - \frac{\hbar}{2}\ddot{Q}_{\rm III}\dot{Q}_{\rm III}^{-2} \right) \right|^2_{x=x_m+i0}. \quad (76)$$

4.2. TUNNELING IONIZATION/RESONANT SCATTERING: COMPLEX ENERGY EIGENVALUES

4.2.1. Exact Solution

By placing a "wall" at $x = x_1$, as depicted in Figure 1(b), the scattering problem is converted to a continuum, resonant scattering problem. A measure of the probability density ratio to find the particle "inside" the confining potential between x_1 and x_m and "outside" where $x > x_m$ is (with a_1, b_1, a_2, b_2 all taken real)

$$\rho_{\rm inside} = \frac{a_1^2 + b_1^2}{a_2^2 + b_2^2}. \quad (77)$$

From the boundary condition at $x = x_1$,

$$\psi_1(x_1) = 0 \quad (78)$$

$$= a_1 {\rm Ai}[\kappa^{-2/3} k(x_1 - x_{c1})] + b_1 {\rm Bi}[\kappa^{-2/3} k(x_1 - x_{c1})], \quad (79)$$

and the matching conditions (9) and (10) or (11) and (12), a straightforward but inelegant expression can be obtained for $\rho_{\rm inside}$, which we do not give here. A plot of $\rho_{\rm inside}$ will be given below in Section 6.2.

We focus instead on the tunneling-ionization picture that results from a second, purely outgoing wave boundary condition at infinity [Eq. (47)] coupled with the zero boundary condition at $x = x_1$. The resulting energy eigenvalues are complex. The complex eigenvalues succinctly parameterize the locations and widths of the continuum resonances. To evaluate $\psi_1(x_1)$, use Eqs. (9), (10), (48), and (49):

$$\psi_1(x_1) = \pi({\rm Bi}[\kappa^{-2/3} k(x_1 - x_{c1})] - i{\rm Ai}[\kappa^{-2/3} k(x_1 - x_{c1})])\kappa^{2/3} \frac{d}{dE} ({\rm Bi}[\kappa^{-2/3}(V_0 - E)]{\rm Ai}[\kappa^{-2/3}(V_0 - E)]) + i\pi {\rm Bi}[\kappa^{-2/3} k(x_1 - x_{c1})]\kappa^{2/3} \frac{d}{dE} {\rm Ai}[\kappa^{-2/3}(V_0 - E)]^2 - \pi {\rm Ai}[\kappa^{-2/3} k(x_1 - x_{c1})]\kappa^{2/3} \frac{d}{dE} {\rm Bi}[\kappa^{-2/3}(V_0 - E)]^2. \quad (80)$$

Equation (78), $\psi_1(x_1) = 0$, with $\psi_1(x_1)$ given by Eq. (80), is an implicit equation to be solved for the complex eigenvalues E.

4.2.2. JWKB Solution

For tunneling ionization, the outgoing wave boundary condition is again Eqs. (55)–(57), namely, $c_{IV} = 1$, $d_{IV} = 0$, which through the connection formulas at x_{c2}, Eqs. (39) and (40), leads to $c_{III} = 1$, $d_{III} = 0$. The zero boundary condition at x_1 is $\psi_1(x_1) = 0$, can be put in the form

$$\sin[S_I(x_1)/\hbar + \pi/4 - \delta_I] = 0 \tag{81}$$

or

$$S_I(x_1)/\hbar + \pi/4 - \delta_I = n\pi, \quad (n = 1, 2, \ldots), \tag{82}$$

where δ_I is defined by [cf. Eq. (13)]

$$e^{-2i\delta_I} = -\frac{c_I}{d_I}. \tag{83}$$

Note that n in Eq. (82) starts with 1, not 0, because

$$S_I^{(0)}(x_1)/\hbar + \pi/4 = \frac{2}{3}k^{1/2}(x_{c1} - x_1)^{3/2}/\hbar + \pi/4 \tag{84}$$

is not close to 0 and δ_I is meant to be small. An appropriate expression for δ_I is required to be able to solve for E.

We already have d_I [cf. Eq. (75)]; we need c_I. From Eq. (37) [$c_I = -id_{II}$], Eq. (44) [d_{II}], again that (c_{III}, d_{III}) = (1, 0), and a slight extension of the argument that led from Eq. (64) to (75),

$$c_I = -\frac{i}{2}\dot{Q}_{II}^{-1/2}e^{Q_{II}/\hbar}(-\dot{Q}_{III})^{-1/2}e^{Q_{III}/\hbar}\left(-\dot{Q}_{III} + \frac{\hbar}{2}\frac{\ddot{Q}_{III}}{\dot{Q}_{III}}\right)\Bigg|_{x=x_m+i0} - \frac{i}{2}\dot{Q}_{II}^{-1/2}\left[e^{Q_{II}/\hbar}\left(+\dot{Q}_{II} - \frac{\hbar}{2}\frac{\ddot{Q}_{II}}{\dot{Q}_{II}}\right)\right] \times (-\dot{Q}_{III})^{-1/2}e^{Q_{III}/\hbar}\Bigg|_{x=x_m+i0}, \tag{85}$$

$$= -ie^{2Q_{III}/\hbar} \times \left(1 - \frac{\hbar}{2}\ddot{Q}_{III}\dot{Q}_{III}^{-2}\right)\Bigg|_{x=x_m+i0} + \frac{\hbar}{2}\ddot{Q}_{III}\dot{Q}_{III}^{-2}\Bigg|_{x=x_m+i0}, \tag{86}$$

$$= -d_I + \frac{\hbar}{2}\ddot{Q}_{III}\dot{Q}_{III}^{-2}\Bigg|_{x=x_m+i0}. \tag{87}$$

Then, δ_I can be evaluated from

$$\tan\delta_I = i\frac{c_I + d_I}{c_I - d_I} \tag{88}$$

$$= 1/\left(2e^{2Q_{III}/\hbar} - i - \frac{4e^{2Q_{III}/\hbar}}{\hbar\ddot{Q}_{III}\dot{Q}_{III}^{-2}}\right)_{x=x_m+i0}. \tag{89}$$

In such a way we obtain the "quantization condition" for the complex energy resonance eigenvalues,

$$S_I(x_1)/\hbar - \arctan\left[1/\left(2e^{2Q_{III}/\hbar} - i - \frac{4e^{2Q_{III}/\hbar}}{\hbar\ddot{Q}_{III}\dot{Q}_{III}^{-2}}\right)_{x=x_m+i0}\right] = \left(n - \frac{1}{4}\right)\pi, \qquad (n = 1, 2, \ldots). \tag{90}$$

4.3. DOUBLE WELL

4.3.1. Exact Solution

By symmetrically placing a second wall at $x = x_2$, the resonant scattering/tunneling ionization problem is converted into a double-well problem, as depicted in Figure 1(c), with the right boundary condition,

$$\psi_2(x_2) = 0 \tag{91}$$

$$= a_2\mathrm{Ai}[\kappa^{-2/3}k(x_{c2} - x_2)] + b_2\mathrm{Bi}[\kappa^{-2/3}k(x_{c2} - x_2)]. \tag{92}$$

If we take

$$b_2 = \mathrm{Ai}[\kappa^{-2/3}k(x_{c2} - x_2)] \tag{93}$$

$$a_2 = -\mathrm{Bi}[\kappa^{-2/3}k(x_{c2} - x_2)], \tag{94}$$

and use the symmetry (by definition)

$$x_2 - x_{c2} = x_{c1} - x_1, \tag{95}$$

then, instead of Eq. (80), we get for $\psi_1(x_1)$

$$\psi_1(x_1) = 2\pi\mathrm{Ai}[\kappa^{-2/3}k(x_1 - x_{c1})]\mathrm{Bi}[\kappa^{-2/3}k(x_1 - x_{c1})] \times \kappa^{2/3}\frac{d}{dE}(\mathrm{Bi}[\kappa^{-2/3}(V_0 - E)]\mathrm{Ai}[\kappa^{-2/3}(V_0 - E)])$$

$$- \pi \mathrm{Bi}[\kappa^{-2/3}k(x_1 - x_{c1})]^2 \kappa^{2/3} \frac{d}{dE} \mathrm{Ai}[\kappa^{-2/3}(V_0 - E)]^2$$

$$- \pi \mathrm{Ai}[\kappa^{-2/3}k(x_1 - x_{c1})]^2 \kappa^{2/3} \frac{d}{dE} \mathrm{Bi}[\kappa^{-2/3}(V_0 - E)]^2 \tag{96}$$

$$= -2\pi\kappa^{2/3}(\mathrm{Bi}[\kappa^{-2/3}k(x_1 - x_{c1})]\mathrm{Ai}[\kappa^{-2/3}(V_0 - E)] - \mathrm{Ai}[\kappa^{-2/3}k(x_1 - x_{c1})]\mathrm{Bi}[\kappa^{-2/3}(V_0 - E)]) \times \left(\mathrm{Bi}[\kappa^{-2/3}k(x_1 - x_{c1})] \frac{d}{dE} \mathrm{Ai}[\kappa^{-2/3}(V_0 - E)] - \mathrm{Ai}[\kappa^{-2/3}k(x_1 - x_{c1})] \frac{d}{dE} \mathrm{Bi}[\kappa^{-2/3}(V_0 - E)]\right). \tag{97}$$

The equation $\psi_1(x_1) = 0$ now has two sets of roots: The first set are the zeros of the first major factor in Eq. (97) and correspond to the odd (antisymmetric) solutions; the second set are the zeros of the second major factor and correspond to the even (symmetric) solutions. The energy difference between these two solutions is "exponentially small." The numerical results for the three pairs of levels below the maximum of the barrier, with the parameterization (as above) $k = 300$, $x_1 = 0$, $x_m = 1$, and $V_0 = k$, and in addition with $x_2 = 2$, are discussed in Section 6.3.

4.3.2. JWKB Solution

For the symmetric double well, we take a shortcut (possible also in the exact case) by noting that, because the eigenfunctions are either antisymmetric or symmetric, either the wave function or its derivative vanishes at $x = x_m + i0$. In the antisymmetric case we have

$$c_{\mathrm{II}} = -\dot{Q}_{\mathrm{II}}^{-1/2}(x_m) e^{-Q_{\mathrm{II}}(x_m)/\hbar} \tag{98}$$

$$d_{\mathrm{II}} = \dot{Q}_{\mathrm{II}}^{-1/2}(x_m) e^{Q_{\mathrm{II}}(x_m)/\hbar} \tag{99}$$

$$\tan \delta_{\mathrm{I}} = i \frac{c_{\mathrm{I}} + d_{\mathrm{I}}}{c_{\mathrm{I}} - d_{\mathrm{I}}} \tag{100}$$

$$= \frac{1}{i - 2d_{\mathrm{II}}/c_{\mathrm{II}}} \tag{101}$$

$$= \frac{1}{2e^{Q_{\mathrm{II}}(x_m + i0)/\hbar} + i}, \tag{102}$$

while in the symmetric case we obtain

$$c_{\mathrm{II}} = -\dot{Q}_{\mathrm{II}}^{-1/2} e^{-Q_{\mathrm{II}}/\hbar} \frac{\dot{Q}_{\mathrm{II}}}{\hbar} \left(-1 - \frac{\hbar}{2} \ddot{Q}_{\mathrm{II}} \dot{Q}_{\mathrm{II}}^{-2}\right)_{x = x_m + i0} \tag{103}$$

$$d_{\mathrm{II}} = \dot{Q}_{\mathrm{II}}^{-1/2} e^{Q_{\mathrm{II}}/\hbar} \frac{\dot{Q}_{\mathrm{II}}}{\hbar} \left(1 - \frac{\hbar}{2} \ddot{Q}_{\mathrm{II}} \dot{Q}_{\mathrm{II}}^{-2}\right)_{x = x_m + i0} \tag{104}$$

$$\tan \delta_{\mathrm{I}} = 1 \Big/ \left(-2e^{Q_{\mathrm{II}}/\hbar} \frac{1 - \frac{\hbar}{2} \ddot{Q}_{\mathrm{II}} \dot{Q}_{\mathrm{II}}^{-2}}{1 + \frac{\hbar}{2} \ddot{Q}_{\mathrm{II}} \dot{Q}_{\mathrm{II}}^{-2}} + i\right)_{x = x_m + i0}. \tag{105}$$

In either case, the implicit equation to solve for the eigenvalues E is the "quantization condition" Eq. (106) with the appropriate δ_{I} from either Eq. (102) or (105):

$$S_{\mathrm{I}}(x_1)/\hbar - \delta_{\mathrm{I}} = \left(n - \frac{1}{4}\right)\pi, \qquad (n = 1, 2, \ldots). \tag{106}$$

5. Borel Sum Approximants

We calculate what we shall call "Borel sum approximants" by the method of Álvarez et al. [6]. The steps are: (1) Truncate the JWKB series at order $2N_T$ in $\hbar$; (2) divide each $\hbar^{\mathrm{M}}$-term by $M!$; (3) form a Padé approximant, for which we choose to have numerator and denominator degrees both equal N_T; if the series is even and N_T is odd, then the numerator and denominator degrees should be $N_T - 1$ and $N_T + 1$, respectively (both numerator and denominator in that case have to be polynomials in $\hbar^2$); (4) resolve the Padé approximant into partial fractions; (5) replace $\hbar$ by $\hbar t$, multiply by e^{-t}, and integrate. Note that

$$\int_0^\infty e^{-t} \frac{1}{t - r} \, dt = e^{-r}\Gamma[0, -r], \qquad \arg r \neq 0 \tag{107}$$

$$= e^{-r}[-\mathrm{Ei}(r) \pm \pi i], \qquad 0 < \pm \arg r < \pi. \tag{108}$$

In this way the JWKB series for $S(x)$ and $Q(x)$, through order $\hbar^{2\mathrm{N_T}}$, are numerically calculated by Borel sum approximants that are a sum of N_T (or $N_T + 1$) incomplete gamma functions plus a constant. It is straightforward to carry out this procedure using Mathematica [7].

Equation (108) explicitly displays the discontinuity of the incomplete gamme function when r falls on the positive real axis, which is implicit in Eq. (107). As an exercise, one can verify numerically that [with Eq. (23) and with $\hbar = 1$]

$$\lim_{N_T \to \infty} 2e^{\text{Borel sum appoximant}(N_T) \text{ of } 2Q_{\text{II}}(x \pm i0)} = \text{Bi}(x)/\text{Ai}(x) \mp i. \tag{109}$$

The fact that the imaginary part is $\mp i$ is true in general and does not depend on the explicit Airy function case considered here.

6. Numerical Results

All the numerical examples reported here have in common the parameters $\hbar = 2m = 1$ and $k = V_0 = 300$. The boundaries and matching point are taken to be $x_1 = 0$, $x_m = 1$, and $x_2 = 2$. The transmission coefficient is independent of x_1, x_m, and x_2 but dependent on k and $E - V_0$.

6.1. TRANSMISSION COEFFICIENT

The exact transmission coefficient [Eq. (53)] and the JWKB transmission coefficient for $E > V_0$ [Eq. (63)] and for $E < V_0$ [Eq. (76)] are to be compared.

6.1.1. Simple Illustration: $E > C_0$, JWKB Through Fourth Order in $\hbar$

It is instructive to examine the calculation of $1/T_{\text{JWKB}}$ when $E > V_0$ [Eq. (63)] one step at a time. Through fourth order in $\hbar$, with $2m = 1$, and ζ_{I} shortened to ζ,

$$1/T_{\text{JWKB}} = 1 + \frac{\hbar^2}{36\zeta^2} - \frac{35\hbar^4}{1296\zeta^4} + O(\hbar^6) \tag{110}$$

Borel transform $(1/T_{\text{JWKB}})$

$$= 1 + \frac{\hbar^2}{72\zeta^2} - \frac{35\hbar^4}{31104\zeta^4} + O(\hbar^6) \tag{111}$$

Padé approximant [2, 2]

$$\text{of Borel transform } (1/T_{\text{JWKB}}) = \frac{1 + \dfrac{41\hbar^2}{432\zeta^2}}{1 + \dfrac{35\hbar^2}{432\zeta^2}}. \tag{112}$$

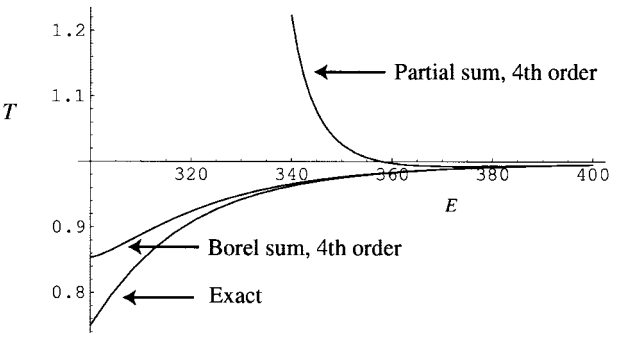

FIGURE 3. Transmission coefficient T when $k = V_0 = 300$ and $\hbar = 2m = 1$: exact, JWKB through $\hbar^4$; and Borel sum approximant of JWKB through $\hbar^4$.

Replace $\hbar$ by $\hbar t$ in this last equation; the denominator has two purely imaginary roots $t_{\pm}$:

$$t_{\pm} = \pm i \sqrt{\frac{432\zeta^2}{35\hbar^2}} \approx \pm 3.51324 i \frac{\zeta}{\hbar}. \tag{113}$$

Multiply by e^{-t} and integrate to obtain the corresponding Borel sum approximant:

$$\text{Borel sum approximant } [2, 2]\,(1/T_{\text{JWKB}}) = \frac{41}{35} + 0.30113 i \frac{\zeta}{\hbar}\left(e^{-i3.51324\zeta/\hbar}\Gamma[0, -i3.51324\zeta/\hbar] - e^{i3.51324\zeta/\hbar}\Gamma[0, i3.51324\zeta/\hbar]\right). \tag{114}$$

In Figure 3 we plot the exact transmission coefficient along with the two approximations that are the reciprocals of Eqs. (110) and (114) with parameters $\hbar = 2m = 1$ and $k = V_0 = 300$. Note that the partial sum is useless when $E < 358.2$ and that the Borel sum approximant is reasonable here even at $E - V_0 = 0$. The nature of the asymptotic expansion is that it is accurate near $\hbar = 0$, which is equivalent to E near infinity. In this case, the fourth-order JWKB partial sum is only accurate where $T \approx 1$, while T is interesting primarily when it is not near 0 or 1.

6.1.2. Why for $E > V_0$, When E is Near V_0, Partial-Sum JWKB Gets Worse, While Borel Sum JWKB Gets Better, as the Order with Respect to $\hbar$ Increases

Equations (110) and (114) illustrate another fact: The formula for $1/T_{\text{JWKB}}$ is singular like ζ_{I}^{-2N}, where N is the JWKB order, the highest power of $\hbar^2$,

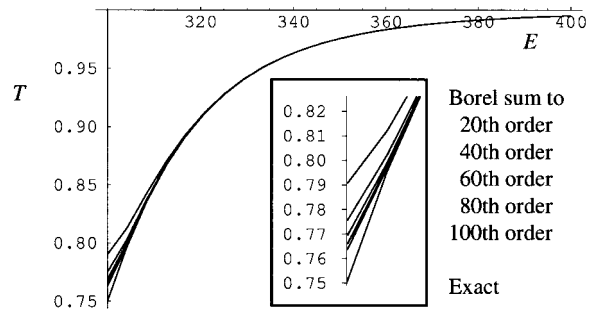

FIGURE 4. Transmission coefficient T when $E \geq V_0 = k = 300$ and $\hbar = 2m = 1$ for $E = 300$–400: exact; and Borel sum approximant of JWKB through $\hbar^N$, with $N = 20$, 40, 60, 80, and 100. Inset: magnification of region near $E = 300$.

and $\zeta_I = (2/3k)(E - V_0)^{3/2}$. As N increases, the region of usefulness of the JWKB partial sum moves to larger E, toward ∞, where $T = 1$. On the other hand, the behavior of the Borel sum approximant of $1/T_{\text{JWKB}}$ depends on $\zeta\Gamma[0, c\zeta]$ as $\zeta \to 0$, and

$$\lim_{\zeta \to 0} \zeta\Gamma[0, c\zeta] = 0. \tag{115}$$

Consequently, the Borel sum approximants of $1/T_{\text{JWKB}}$ stay finite as E approaches V_0 from above.

6.1.3. High-Order JWKB for T When $E > V_0$

In Figure 4 we plotted (from top to bottom) the Borel sum approximants of the JWKB transmission coefficient [Eq. (63)] to orders 20, 40, 60, 80, and 100 in $\hbar$. The lowest curve is the exact T [Eq. (53)]. The JWKB–Borel curves converge toward the exact, even at $E = V_0$, where $T_{\text{exact}} = 3/4$.

6.1.4. JWKB for T When $E < V_0$

For $E < V_0$, it is necessary to construct Borel sum approximants for Eq. (76). We explored several strategies.

Note that the expression $[1 - (\hbar/2)\ddot{Q}_{\text{III}}\dot{Q}_{\text{III}}^{-2}]$, except for the "1," involves odd powers of $\hbar$. Direct Borel sum approximants with the intermediate Padé numerator one degree less than the denominator will lead to an expression for $1/T$ that goes to 0 as $V_0 - E \to 0$ and therefore the calculated $T \to \infty$. Consequently, the convergence as $V_0 - E \to 0$ is highly nonuniform.

By taking the logarithm we can shift the odd series into the exponential,

$$1/T_{\text{JWKB}} = \left|\exp\left\{\left[2Q_{\text{III}} + \hbar \log\left(1 - \frac{\hbar}{2}\ddot{Q}_{\text{III}}\dot{Q}_{\text{III}}^{-2}\right)\right]/\hbar\right\}\right|^2. \tag{116}$$

Borel sum approximants of the expression in square brackets can be taken to even powers of $\hbar$. Nevertheless, the final Borel sum approximants are similar to Eq. (114) times an extra factor of ζ, which therefore approaches 0 as $\zeta \to 0$. Consequently, the calculated $T \to 1$, which is not as bad as ∞. The calculated values of T are useful closer to $V_0 - E = 0$.

The best strategy is to keep only $2Q_{\text{III}}^{(0)}/\hbar = 2\zeta_{\text{III}}/\hbar$ in the exponential, expand $\exp[2(Q_{\text{III}} - Q_{\text{III}}^{(0)})/\hbar]$ out of the exponential, combine it with $[1 - (\hbar/2)\ddot{Q}_{\text{III}}\dot{Q}_{\text{III}}^{-2}]$, and Borel sum the product. The end result is that the exponential factor approaches 1, while the even-order Borel sum approximants of the power series factor approach nonzero, finite constants. The process even appears to converge toward the exact value of T (=3/4) at $E = V_0$. In Figure 5, the transmission coefficient is plotted for Borel sum approximants with $\hbar$ truncation orders 20, 40, and 56, along with the exact curve. For comparison, the JWKB fourth-order partial sum departs from the exact curve visibly around $E = 250$.

For both $E < V_0$ and $E > V_0$, the JWKB method with Borel summation accurately reproduces the exact transmission coefficient.

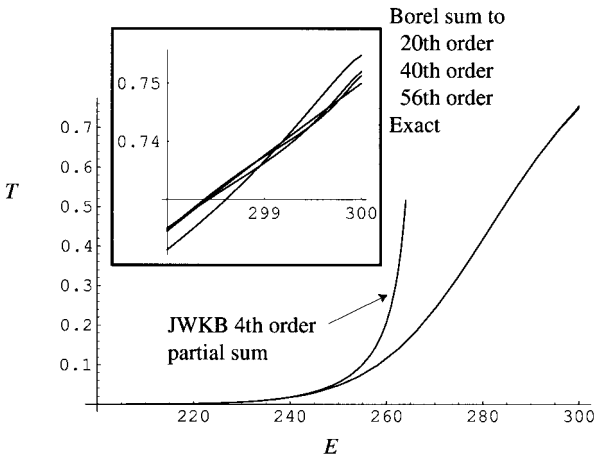

FIGURE 5. Transmission coefficient T when $E \leq V_0 = k = 300$ and $\hbar = 2m = 1$ for $E = 200$–300: exact; and Borel sum approximant of JWKB through $\hbar^N$, with $N = 20$, 40, and 56. Inset: magnification of region from $E = 298$–300.

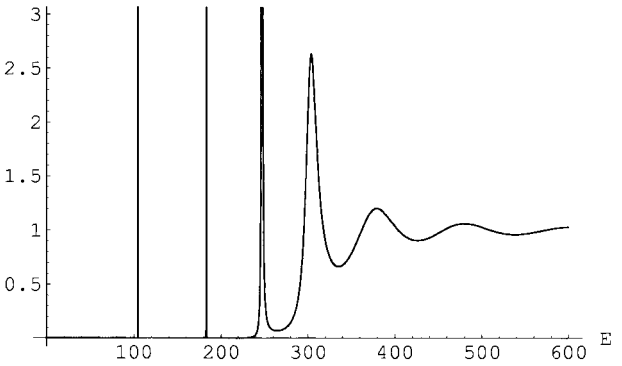

FIGURE 6. Relative probability density [Eq. (77)] to be inside the confining potential as a function of E, when $\hbar = 2m = 1$, $k = 300$, $x_1 = 0$, $x_m = 1$, and $V_0 = k$. The sharp peaks near 105, 183, and 247 have been truncated.

6.2. TUNNELING IONIZATION

6.2.1. Resonance Scattering Picture

Figure 6 shows a plot of the relative probability density ρ_{inside} for the particle inside the well, discussed in Section 4.2.1. The parameter values are $\hbar = 2m = 1$, $k = V_0 = 300$, $x_1 = 0$, and $x_m = 1$. Three resonances fall below the maximum of the potential at 300: near 105, 183, and 247. The exact locations and widths of the resonances are given in Table I. The maxima are off-scale in the figure.)

6.2.2. Complex Eigenvalue/Tunneling Ionization Picture

The exact complex energy eigenvalues were obtained by solving Eqs. (78) and (80) using the "FindRoot" command of Mathematica [7] and are reported in columns 4 and 5 of Table I. The agreement with the resonance positions and widths reported in columns 2 and 3 is as expected.

6.2.3. Raw Convergence of Borel Sum Approximants for $S_{\text{I}}(x_1)$ and $Q_{\text{III}}(x_m)$

To solve the JWKB quantization condition (90) note that two independent quantities need to be calculated: $S_{\text{I}}(x_1)$ and δ_{I}, the latter of which depends on $Q_{\text{III}}(x_m + i0)$. We first discuss convergence of S_{I} and Q_{III}. To achieve a given accuracy, the truncation orders do not have to be the same and depend, respectively, on the values of $\zeta_{\text{I}}(x_1, k, x_{c1})$ and $\zeta_{\text{III}}(x_m + i0, k, x_{c2})$ or, more transparently, E and $V_0 - E$. If $|E|$ is small and $|V_0 - E|$ large, more terms are needed for $S_{\text{I}}(x_1)$ than for $Q_{\text{III}}(x_m + i0)$, and the reverse if the order is reversed. The raw convergence rates are illustrated in Table II, which lists the values of $S_{\text{I}}^{(N)}(x_1)$, $Q_{\text{III}}^{(N)}(x_m)$, and the increments of successive Borel sum approximants for $E = 105$, 183, and 247. One can easily see from the table the dependence of the rate of divergence of the JWKB series on ζ_{I} and ζ_{III} and the ease or difficulty with which the Borel method accordingly converges. The worst case given is $Q_{\text{III}}(x_m)$ for $E = 247$, for which the "large" parameter ζ_{III} is only 0.857 and for which the Borel sum approximants labor to converge.

6.2.4. Convergence of Eigenvalues, Calculated as Roots of Implicit Equations

The eigenvalues are *not calculated directly* by Borel summation. First, S and Q are calculated by Borel sum approximants, explicitly as a function of E. These are then used to solve the *implicit* Eq. (90) for the eigenvalues.

The convergence of the JWKB values for the complex resonance eigenvalues, calculated indirectly by the Borel sum approximant method, are illustrated in Table III (the exact eigenvalues are in Table I). Table III is best studied with the aid of Table II. The important points are:

TABLE I

Resonance positions and widths (half-width at half-maximum) for resonant-scattering boundary condition: $\psi_1(x_1) = 0$, $x_1 = 0$, $x_m = 1$, E real, $k = 300$, and $V_0 = k$, compared with complex-energy eigenvalues for outgoing-wave boundary condition.

Resonance number n	Resonance position and half-width		Complex energy eigenvalue	
	E_n	δE_n	Re E_n	$-$Im E_n
1	104.7800542616973850	$2.163331588 \times 10^{-10}$	104.7800542616974016	$2.163331575 \times 10^{-10}$
2	183.1949242807618887	$7.589955977 \times 10^{-5}$	183.1949242803536993	$7.589955976 \times 10^{-5}$
3	247.0578387411503412	0.170604580	247.0564298845948887	0.170567133

TABLE II

Convergence of partial sums and Borel sum approximants: $x_1 = 0$, $x_m = 1$, E real, $k = 300$, and $V_0 = k$.

E	N	ζ_{I}	$S_{\mathrm{I}}^{(N)}(x_1)$	ΔBorel sum-$S_{\mathrm{I}}(x_1)$	ζ_{III}	$Q_{\mathrm{III}}^{(N)}(x_m)$	ΔBorel sum-$Q_{\mathrm{III}}(x_m)$
105	1	2.391	-29×10^{-3}	27225×10^{-6}	6.051	114762×10^{-7}	11610721×10^{-9}
	2		3×10^{-3}	352×10^{-6}		1603×10^{-7}	31825×10^{-9}
	3		-1×10^{-3}	172×10^{-6}		137×10^{-7}	16987×10^{-9}
	4		2×10^{-3}	115×10^{-6}		29×10^{-7}	8390×10^{-9}
	5		-5×10^{-3}	50×10^{-6}		11×10^{-7}	384×10^{-9}
	6		19×10^{-3}	38×10^{-6}		7×10^{-7}	273×10^{-9}
	7		-109×10^{-3}	3×10^{-6}		6×10^{-7}	46×10^{-9}
	8					8×10^{-7}	25×10^{-9}
	9					13×10^{-7}	6×10^{-9}
	10					27×10^{-7}	3×10^{-9}
	11					69×10^{-7}	1×10^{-9}
183	1	5.501	-126233×10^{-7}	$124551526 \times 10^{-10}$	2.812	247×10^{-4}	26238×10^{-6}
	2		2134×10^{-7}	368359×10^{-10}		16×10^{-4}	452×10^{-6}
	3		-220×10^{-7}	76583×10^{-10}		6×10^{-4}	581×10^{-6}
	4		56×10^{-7}	19197×10^{-10}		6×10^{-4}	658×10^{-6}
	5		-26×10^{-7}	1065×10^{-10}		11×10^{-4}	120×10^{-6}
	6		20×10^{-7}	348×10^{-10}		31×10^{-4}	131×10^{-6}
	7		-22×10^{-7}	20×10^{-10}		132×10^{-4}	32×10^{-6}
	8		32×10^{-7}	6×10^{-10}		762×10^{-4}	26×10^{-6}
	9					5797×10^{-4}	9×10^{-6}
	10					56180×10^{-4}	6×10^{-6}
	11					675858×10^{-4}	3×10^{-6}
247	1	8.626	-8050161×10^{-9}	$8005702438009 \times 10^{-15}$	0.857	8×10^{-2}	1167×10^{-4}
	2		55341×10^{-9}	$9959938395 \times 10^{-15}$		6×10^{-2}	132×10^{-4}
	3		-2323×10^{-9}	$1060131546 \times 10^{-15}$		24×10^{-2}	132×10^{-4}
	4		240×10^{-9}	$134153176 \times 10^{-15}$		250×10^{-2}	263×10^{-4}
	5		-46×10^{-9}	2828359×10^{-15}		4824×10^{-2}	152×10^{-4}
	6		14×10^{-9}	494769×10^{-15}		148792×10^{-2}	209×10^{-4}
	7		-6×10^{-9}	18664×10^{-15}		6712513×10^{-2}	96×10^{-4}
	8		4×10^{-9}	3261×10^{-15}		416888200×10^{-2}	99×10^{-4}
	9		-3×10^{-9}	262×10^{-15}		$34110764869 \times 10^{-2}$	51×10^{-4}
	10		3×10^{-9}	52×10^{-15}		$3556424699882 \times 10^{-2}$	49×10^{-4}
	11		-4×10^{-9}	6×10^{-15}		$460277849406854 \times 10^{-2}$	27×10^{-4}
	12		6×10^{-9}	1×10^{-15}			

		$S_{\mathrm{I}}(x_1)$			$Q_{\mathrm{III}}(x_m)$	
E	N_S	Exact	Borel sum to N_S terms	N_Q	Exact	Borel sum to N_Q terms
105	7	2.363780	2.363778	11	$6.062825636 + i1.3547 \times 10^{-6}$	$6.062825635 + i1.3543 \times 10^{-6}$
183	8	5.4888567305	5.4888567306	11	$2.839173 + i0.000855$	$2.839173 + i0.000854$
247	12	8.618469084064061	8.618469084064061	11	$0.9340 + i0.0386$	$0.9348 + i0.0371$

ΔBorel sum-$S_{\mathrm{I}}(x_1) = |\text{Borel sum-}\sum_{j=0}^{N} S_{\mathrm{I}}^{(j)}(x_1) - \text{Borel sum-}\sum_{j=0}^{N-1} S_{\mathrm{I}}^{(j)}(x_1)|$. Similarly for ΔBorel sum-$Q_{\mathrm{III}}(x_m)$.

1. For all three eigenvalues, obtained as roots of Eq. (90) using Borel sum approximants for S and Q, there is numerical convergence. This is *the* most important point. The rest are details.
2. In the case of E_1, $\zeta_{\mathrm{III}} \approx 6.051$ is relatively large so that the truncation level N_Q for Q is much lower than N_S for S, for which $\zeta_{\mathrm{I}} \approx 2.391$. Moreover, the effects of Q and S seem relatively independent, one primarily affecting the imaginary part and the other the real part.

TABLE III

Numerical convergence of Borel sum approximant method for complex resonance eigenvalues obtained by solving Eq. (90) with $x_1 = 0$, $x_m = 1$, $k = 300$, and $V_0 = k$ when $S_I(x_1)$ is calculated as a Borel sum approximant to N_S terms and $Q_{III}(x_m + i0)$ and $\ddot{Q}_{III}\dot{Q}_{III}^{-2}(x_m + i0)$ are calculated as Borel sum approximants to N_Q terms.

$E_1(N_S, N_Q) - E_1$(exact)				$E_2(N_S, N_Q) - E_2$(exact)				$E_3(N_S, N_Q) - E_3$(exact)			
N_S	N_Q	Re	Im	N_S	N_Q	Re	Im	N_S	N_Q	Re	Im
24	6	-45×10^{-12}	1903×10^{-16}	16	2	-999393×10^{-12}	-4295549×10^{-12}	6	2	500×10^{-6}	26558×10^{-6}
24	7	-45×10^{-12}	323×10^{-16}	16	3	-2644412×10^{-12}	-1955470×10^{-12}	6	3	7016×10^{-6}	21112×10^{-6}
24	8	-45×10^{-12}	-230×10^{-16}	16	4	-177095×10^{-12}	619438×10^{-12}	6	4	10513×10^{-6}	1474×10^{-6}
24	9	-45×10^{-12}	37×10^{-16}	16	5	-568722×10^{-12}	83691×10^{-12}	6	5	5366×10^{-6}	11905×10^{-6}
24	10	-45×10^{-12}	19×10^{-16}	16	6	129584×10^{-12}	-25422×10^{-12}	6	6	2603×10^{-6}	-3871×10^{-6}
24	11	-45×10^{-12}	-17×10^{-16}	16	7	14214×10^{-12}	105085×10^{-12}	6	7	4741×10^{-6}	3267×10^{-6}
24	12	-45×10^{-12}	2×10^{-16}	16	8	-11658×10^{-12}	-30650×10^{-12}	6	8	-746×10^{-6}	-2096×10^{-6}
25	12	35×10^{-12}	2×10^{-16}	16	9	25132×10^{-12}	-1479×10^{-12}	6	9	2736×10^{-6}	-127×10^{-6}
26	12	-14×10^{-12}	2×10^{-16}	16	10	-8507×10^{-12}	2977×10^{-12}	6	10	-1029×10^{-6}	-439×10^{-6}
27	12	11×10^{-12}	2×10^{-16}	16	11	873×10^{-12}	-6890×10^{-12}	6	11	1062×10^{-6}	-891×10^{-6}
28	12	-5×10^{-12}	2×10^{-16}	16	12	448×10^{-12}	2685×10^{-12}	6	12	-559×10^{-6}	199×10^{-6}
				16	13	-1922×10^{-12}	-829×10^{-12}	6	13	171×10^{-6}	-709×10^{-6}
				16	14	890×10^{-12}	105×10^{-12}	6	14	-172×10^{-6}	283×10^{-6}
				16	15	-477×10^{-12}	491×10^{-12}	6	15	-145×10^{-6}	-373×10^{-6}
				16	16	146×10^{-12}	-276×10^{-12}	6	16	18×10^{-6}	190×10^{-6}
				16	17	86×10^{-12}	225×10^{-12}	6	17	-185×10^{-6}	-133×10^{-6}
				16	18	-69×10^{-12}	-91×10^{-12}	6	18	73×10^{-6}	86×10^{-6}
				16	19	88×10^{-12}	11×10^{-12}	6	19	-133×10^{-6}	-9×10^{-6}
				16	20	-43×10^{-12}	6×10^{-12}	6	20	66×10^{-6}	20×10^{-6}
				16	21	21×10^{-12}	-27×10^{-12}	6	21	-71×10^{-6}	36×10^{-6}
				16	22	-7×10^{-12}	16×10^{-12}	6	22	41×10^{-6}	-11×10^{-6}
				16	23	-4×10^{-12}	-13×10^{-12}	6	23	-27×10^{-6}	40×10^{-6}
				16	24	4×10^{-12}	6×10^{-12}	6	24	19×10^{-6}	-19×10^{-6}
								6	25	-3×10^{-6}	30×10^{-6}
								6	26	5×10^{-6}	-16×10^{-6}
								6	27	7×10^{-6}	18×10^{-6}
								6	28	-2×10^{-6}	-11×10^{-6}

The exact values of the complex eigenvalues are in Table I.

One can see this in the first set of columns in Table III, where first N_Q is varied, then second N_S.

3. In the case of E_2, $\zeta_{\mathrm{I}} \approx 5.501$ is relatively large, so that the truncation level N_S for S is lower than N_Q for Q, for which $\zeta_{\mathrm{III}} \approx 2.812$. We chose the value $N_S = 16$, which is sufficiently large to achieve absolute accuracy better than 1×10^{-13}, and we let N_Q increase from 2 to 24. The accuracy of both the real and imaginary parts is determined by N_Q.
4. In the case of E_3, $\zeta_{\mathrm{I}} \approx 8.626$ is so large, and $\zeta_{\mathrm{III}} \approx 0.857$ so small, that convergence is completely dominated by N_Q. For N_S we take the modest value 6, which should be sufficient to achieve absolute accuracy better than 1×10^{-7} [cf. Table II], and let N_Q increase from 2 to 28. Although the method converges, the rate is slow.

6.3. DOUBLE WELL

6.3.1. Exponentially Small Splitting

While tunneling ionization tests the JWKB method with a complex boundary condition, the double well is even more interesting because the separations between paired energy levels (for $E < V_0$) are exponentially small. This is best understood in the large-Q limit, where Eqs. (106), (105), and (102) become

$$S_{\mathrm{I}}(x_1)/\hbar \mp \frac{1}{2} e^{-Q_{\mathrm{II}}/\hbar} \approx \left(n - \frac{1}{4}\right)\pi, \qquad (n = 1, 2, \ldots). \quad (117)$$

6.3.2. Exact Double-Well Eigenvalues

The exact double-well energies are reported in the last line of Table IV, from which it can be seen that the separations of the paired energies are 0.00015844372, 0.08193372687, and 3.59612141877, respectively. (One might observe about 3.59612141877 that *theoretically* exponentially small is not necessarily *numerically* exponentially small.)

6.3.3. JWKB–Borel Energies

As is the case for the complex eigenvalues, the S and Q are obtained by Borel sum approximants explicitly as a function of E. The energy eigenvalues are then obtained as the roots of Eq. (106), with δ_{I} taken from Eq. (102) or (105).

The convergence of the JWKB Borel sum double-well energies is reported in Table IV. The lowest-energy pair is dominated by the convergence of S. Not only does Q converge faster, but its influence is small (in the numerically exponentially small sense). For the second and third pairs, calculation of Q dominates the convergence. In the case of the third pair, the convergence is so slow that it was only practical to achieve absolute accuracy 3×10^{-6}, compared with the easy 1×10^{-11} for the first two pairs.

Note that to the extent the limit in Eq. (109) is not reached the calculated energy eigenvalues will have artifactual imaginary parts; they are in general the same order of magnitude or less than the *error* in the real parts of the calculated energies. Because the limits of the imaginary parts are 0, we did not report them in Table IV.

The antisymmetric partner of each double-well pair vanishes at $x = x_m$. Consequently, it is also the solution of a single-well problem with the second boundary point at x_m.

As for the complex resonance eigenvalues, the important result is that, within the limitations of rate of convergence, the JWKB–Borel method leads to exact eigenvalues.

7. Conclusion

Three topologically identical two-linear-turning-point problems, which differ only in their boundary conditions, have been solved exactly and by JWKB expansion. The Borel sum approximants of the JWKB expansion converge to the transmission coefficient T and give eigenvalues for tunneling ionization and for the double well that converge numerically toward the exact eigenvalues, as presented in Figure 2 and Tables III and IV. The connection formulas at the linear turning points (see footnote in Section 3.2), Eqs. (33)–(36) and Eqs. (37)–(40), play an essential role in communicating the left boundary condition to the right and vice versa. The inescapable conclusions are that calculations done by the JWKB method with Borel summation give exact solutions, that is, JWKB calculation can be carried out to as high an accuracy as computers permit, with practical limitations coming from numerical precision and from the slow rate of convergence if a "ζ" is small. Not only are

TABLE IV

Numerical convergence of the Borel sum approximant method for double-well eigenvalues obtained by solving Eqs. (106) and (105) for the symmetric states, and (106) and (102) for the antisymmetric states, with $x_1 = 0$, $x_m = 1$, $x_2 = 2$, $k = 300$, and $V_0 = k$.

$E_1(N_S, N_Q) - E_1$(exact)				$E_2(N_S, N_Q) - E_2$(exact)				$E_3(N_S, N_Q) - E_3$(exact)			
N_S	N_Q	Symmetric	Antisymmetric	N_S	N_Q	Symmetric	Antisymmetric	N_S	N_Q	Symmetric	Antisymmetric
14	6	-3306×10^{-11}	-3306×10^{-11}	14	14	1459×10^{-11}	-1308×10^{-11}	6	15	-1315×10^{-6}	951×10^{-6}
15	6	2567×10^{-11}	2566×10^{-11}	14	15	-753×10^{-11}	686×10^{-11}	6	16	525×10^{-6}	-131×10^{-6}
16	6	-766×10^{-11}	-767×10^{-11}	14	16	224×10^{-11}	-207×10^{-11}	6	17	-819×10^{-6}	1129×10^{-6}
17	6	594×10^{-11}	594×10^{-11}	14	17	152×10^{-11}	-132×10^{-11}	6	18	407×10^{-6}	-438×10^{-6}
18	6	-192×10^{-11}	-192×10^{-11}	14	18	-117×10^{-11}	103×10^{-11}	6	19	-366×10^{-6}	809×10^{-6}
19	6	149×10^{-11}	149×10^{-11}	14	19	144×10^{-11}	-130×10^{-11}	6	20	217×10^{-6}	-396×10^{-6}
20	6	-52×10^{-11}	-52×10^{-11}	14	20	-70×10^{-11}	63×10^{-11}	6	21	-92×10^{-6}	442×10^{-6}
21	6	40×10^{-11}	40×10^{-11}	14	21	33×10^{-11}	-31×10^{-11}	6	22	75×10^{-6}	-255×10^{-6}
22	6	-15×10^{-11}	-15×10^{-11}	14	22	-10×10^{-11}	10×10^{-11}	6	23	32×10^{-6}	177×10^{-6}
23	6	12×10^{-11}	11×10^{-11}	14	23	-8×10^{-11}	6×10^{-11}	6	24	-1×10^{-6}	-124×10^{-6}
24	6	-4×10^{-11}	-5×10^{-11}	14	24	7×10^{-11}	-6×10^{-11}	6	25	67×10^{-6}	27×10^{-6}
25	6	4×10^{-11}	3×10^{-11}	14	25	-9×10^{-11}	8×10^{-11}	6	26	-30×10^{-6}	-37×10^{-6}
				14	26	5×10^{-11}	-5×10^{-11}	6	27	60×10^{-6}	-39×10^{-6}
				14	27	-3×10^{-11}	3×10^{-11}	6	28	-32×10^{-6}	9×10^{-6}
				14	28	1×10^{-11}	-1×10^{-11}	6	29	41×10^{-6}	-56×10^{-6}
								6	30	-25×10^{-6}	26×10^{-6}
								6	31	23×10^{-6}	-50×10^{-6}
								6	32	-15×10^{-6}	27×10^{-6}
								6	33	10×10^{-6}	-35×10^{-6}
								6	34	-7×10^{-6}	22×10^{-6}
								6	35	2×10^{-6}	-21×10^{-6}
								6	36	-2×10^{-6}	14×10^{-6}
								6	37	-2×10^{-6}	-11×10^{-6}
								6	38	1×10^{-6}	8×10^{-6}
								6	39	-3×10^{-6}	-3×10^{-6}
								6	40	2×10^{-6}	3×10^{-6}
E_n(exact)		104.77997504041	104.78013348413			183.15407642491	183.23601015178			245.41620414463	249.01232556340

In each case, $S_I(x_1)$ is calculated as a Borel sum approximant to N_S terms and $Q_{II}(x_m + i0)$ and $\ddot{Q}_{II}\dot{Q}_{II}^{-2}(x_m + i0)$ are calculated as Borel sum approximants to N_Q terms. The (artifactual) imaginary parts of the $E_n(N_S, N_Q)$, which tend to 0, have been omitted: They are in general comparable to or less than the *error* in the real parts, i.e., the numbers reported in this table.

the connection formulas correct, but they are one to one, that is, bidirectional.

References

1. Silverstone, H. J. Phys Rev Lett 1985, 55, 2523.
2. Fröman, N.; Fröman, P. O. J Math Phys 1998, 39, 4417.
3. Dunham, J. L. Phys Rev 1932, 41, 713.
4. Messiah, A. Quantum Mechanics; Temmer, G. M., trans.; North-Holland: Amsterdam, 1961–1962.
5. Silverstone, H. J. In Modern Electronic Structure Theory; Yarkony, D. R. Ed.; World Scientiric: Singapore, 1995; chapter 10, Eqs. (195)–(207).
6. Álvarez, G.; Martín-Mayor, V.; Ruiz-Lorenzo, J. J. J Phys A 2000, 33, 841.
7. Wolfram, S. The Mathematica Book, 4th ed.; Wolfram Media/ Cambridge University Press: Cambridge, UK, 1999.